



ELSEVIER

Contents lists available at ScienceDirect

Chinese Chemical Letters

journal homepage: [www.elsevier.com/locate/ccllet](http://www.elsevier.com/locate/ccllet)

## Quantum interference enhanced thermopower in single-molecule thiophene junctions

Hang Chen<sup>a</sup>, Yaorong Chen<sup>a</sup>, Hewei Zhang<sup>a</sup>, Wenqiang Cao<sup>a</sup>, Chao Fang<sup>a</sup>, Yicheng Zhou<sup>b</sup>, Zongyuan Xiao<sup>a</sup>, Jia Shi<sup>a</sup>, Wenbo Chen<sup>b,\*</sup>, Junyang Liu<sup>a,\*</sup>, Wenjing Hong<sup>a,c,\*</sup>

<sup>a</sup> State Key Laboratory of Physical Chemistry of Solid Surfaces, iChem, College of Chemistry and Chemical Engineering, Xiamen University, Xiamen 361005, China

<sup>b</sup> Shanghai Key Laboratory of Materials Protection and Advanced Materials in Electric Power, Shanghai University of Electric Power, Shanghai 200090, China

<sup>c</sup> Beijing National Laboratory for Molecular Sciences, Beijing 100190, China

### ARTICLE INFO

#### Article history:

Received 8 May 2021

Revised 14 June 2021

Accepted 17 June 2021

Available online 26 June 2021

#### Keywords:

Quantum interference

Thermopower

Thermoelectric device

Single-molecule electronics

Single-molecule junctions

### ABSTRACT

Quantum interference (QI) effects, which offer unique opportunities to widely manipulate the charge transport properties in the molecular junctions, will have the potential for achieving high thermopower. Here we developed a scanning tunneling microscope break junction technique to investigate the thermopower through single-molecule thiophene junctions. We observed that the thermopower of 2,4-TP-SAc with destructive quantum interference (DQI) was nearly twice of 2,5-TP-SAc without DQI, while the conductance of the 2,4-TP-SAc was two orders of magnitude lower than that of 2,5-TP-SAc. Furthermore, we found the thermopower was almost the same by altering the anchoring group or thiophene core in the control experiments, suggesting that the QI effect is responsible for the increase of thermopower. The density functional theory (DFT) calculations are in quantitative agreement with the experimental data. Our results reveal that QI effects can provide a promising platform to enhance the thermopower of molecular junctions.

© 2021 Published by Elsevier B.V. on behalf of Chinese Chemical Society and Institute of Materia Medica, Chinese Academy of Medical Sciences.

Investigations of unique electronic properties resulting from quantum effects through single-molecule junctions offer the essential knowledge for the design of high-performance functional molecular materials and devices [1–5]. Quantum interference (QI) effects, which express a quantum phenomenon in which de Broglie waves of electrons interfere with each other when propagating through discrete molecular orbitals, offer unique opportunities to widely tune charge transport properties through single-molecule junctions, by constructive quantum interference (CQI) to improve conductance or destructive quantum interference (DQI) to suppress conductance [6–7]. To date, various QI effects in charge transport have been investigated, such as QI effect in conjugated molecules, the influence of heteroatom substitution and DQI in the molecular  $\sigma$ -system [5,7–9]. However, the experimental study of QI effects in thermopower still needs some investigation. From the perspective of coherent tunneling limit, the thermopower provides valuable information into charge transport, even allows us to estimate the location of frontier molecular levels relative to the Fermi en-

ergy [10–14]. Therefore, the thermopower offers the unique confirmation for the existence of DQI effect in charge transport through single-molecule junctions.

The combination of conductance and thermopower measurement has revealed that the appearance of DQI in the symmetric  $\sigma$ -orbital system and central six-membered ring system, which will lead to a significant difference in their thermopower as well as the conductance [7,15]. However, compared with the symmetric six-membered ring, incorporating heteroatoms into the central five-membered  $\pi$ -conjugated backbone leads to asymmetrical molecular structure. The asymmetrical five-membered heterocyclic cores provide a diversity of molecular structure and enable an investigation of the interaction effect of QI effects in charge transport through single-molecule junctions [16], yet their thermopower properties remain experimentally unexplored. Yang *et al.* studied that asymmetric five-membered  $\pi$ -system modifies the pattern of DQI within the core of the molecular backbone and promotes charge transport through single-molecule junctions [17]. Among them, thiophene derivatives have been extensively studied owing to their unique optical and electronic properties [18–19]. To understand the structure-properties relation in the central five-membered ring system, it is important to understand the ther-

\* Corresponding authors.

E-mail addresses: wenbochen@shiep.edu.cn (W. Chen), jyliu@xmu.edu.cn (J. Liu), whong@xmu.edu.cn (W. Hong).

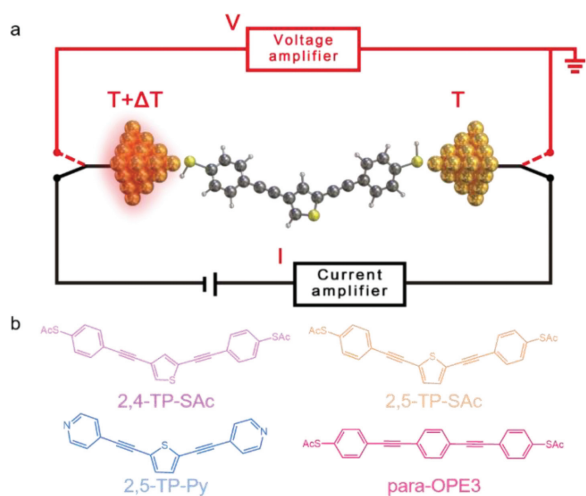


**Fig. 1.** (a) Schematic of the experimental setup. (b) The structures of molecules studied in this work.

mopower and charge transport through thiophene derivatives at the molecular level.

Herein, to explore the role of DQI on thermoelectric properties of the single-molecule junctions, we investigated thermopower and charge transport through single-molecule thiophene junctions by the home-built modified scanning tunneling microscope break junction technique (Fig. 1a) [15,20]. We observed that the thermopower of 2,4-TP-SAc with DQI was nearly twice of 2,5-TP-SAc without DQI, while the conductance of the 2,4-TP-SAc was two orders of magnitude lower than that of 2,5-TP-SAc. Furthermore, we found that the thermopower of 2,5-TP-SAc was almost the same by altering the anchoring group (2,5-TP-Py) or thiophene core (*para*-OPE3) in the control experiment, suggesting that the QI effect is responsible for the increase of thermopower. The experimental results are in quantitative agreement with expectations from density functional theory (DFT) calculations.

The two target molecules 2,4-TP-SAc and 2,5-TP-SAc with acetylthiobenzenes at both ends were shown in Fig. 1b. To verify that the DQI effect is responsible for thermoelectric properties of the single-molecule junctions, we choose 2,5-TP-Py and oligo(phenylene-ethynylene) derivatives with a *para*-connected central phenyl ring (*para*-OPE3) without DQI for the control experiment, which changed the anchoring group and thiophene core, respectively. All target molecules were synthesized according to the previous reports [6,15,17]. Single-molecule conductance measurements were carried out using our home-built scanning tunneling microscope break-junction (STM-BJ) technique in solutions of target molecules in the mixed THF/TMB ( $v/v = 1:4$ ) solvent with the concentration of 0.1 mmol/L [21]. The soft-contact mode, which can prevent direct contact between the tip and the sample to avoid heat transfer during the thermoelectric experiment, was chosen to perform the conductance measurement synchronously [22]. A fixed bias voltage of 0.1 V was added between the tip and the substrate (see Supporting information for more details). The conductance ( $G$ ) versus stretching distance ( $\Delta z$ ) plotted in a semi-logarithmic scale in Fig. 2a shows the typical individual traces of 2,4-TP-SAc, 2,5-TP-SAc, 2,5-TP-Py and *para*-OPE3 with conductance plateaus ranging from  $10^{-5.22} G_0$  to  $10^{-3.38} G_0$  (see Table 1 and Supporting information for more details). Fig. 2b shows the conductance histograms of these molecules with significant conductance peaks, which were constructed from 2000 conductance-distance traces without any selection. These values are consistent with previous studies that used the mechanically controllable break junction (MCBJ) method in their corresponding molecular solutions with hard contact of

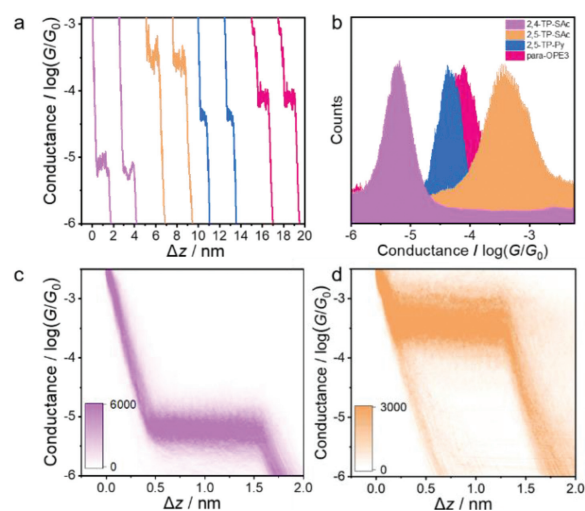


**Fig. 2.** (a) Typical measured conductance distance traces of 2,4-TP-SAc, 2,5-TP-SAc, 2,5-TP-Py and *para*-OPE3. (b) 1D conductance histogram comparisons between 2,4-TP-SAc, 2,5-TP-SAc, 2,5-TP-Py and *para*-OPE3. (c) 2D conductance versus relative distance ( $\Delta z$ ) histogram of 2,4-TP-SAc. (d) 2D conductance versus relative distance ( $\Delta z$ ) histogram of 2,5-TP-SAc.

**Table 1**

Single-molecule Seebeck coefficient and conductance measurements.

Compound	Seebeck coefficient <sup>a</sup> ( $\mu\text{V}/\text{K}$ )	Measured conductance/ $\log(G/G_0)$
2,4-TP-SAc	$+12.36 \pm 0.65$	$-5.22$ (0.467 nS)
2,5-TP-SAc	$+7.97 \pm 0.26$	$-3.38$ (32.3 nS)
2,5-TP-Py	$-7.56 \pm 0.69$	$-4.36$ (3.39 nS)
<i>para</i> -OPE3	$+7.78 \pm 0.34$	$-4.06$ (6.76 nS)

<sup>a</sup> The error bars are based on the standard deviation in the linear fitting of the most probable thermoelectric voltage as a function of  $\Delta T$ .

electrodes [6]. It can be seen that the conductance of the 2,4-TP-SAc (0.467 nS) with DQI was nearly two orders of magnitude lower than that of the 2,5-TP-SAc (32.3 nS) without DQI, although both of them have almost the same length. The comparison suggests that the DQI effect can significantly tune charge transport through single-molecule junctions. Also, the results reveal that the charge transport can also be tuned by altering the thiophene core (*para*-OPE3) and end group (2,5-TP-Py). The plateaus and peaks were further verified by a clear density cloud in the corresponding 2D conductance-distance histograms, containing all the traces from single-molecule junction and the tunneling traces, as shown in Fig. 2c for 2,4-TP-SAc and Fig. 2d for 2,5-TP-SAc.

To further investigate the relationship between DQI and heat transport properties, we used the same STM-BJ to measure the thermopower of the single-molecule junction at room temperature [20]. To measure the thermopower of single-molecule junctions, a stable temperature difference ( $\Delta T = T_{\text{substrate}} - T_{\text{tip}}$ ) between the tip (at room temperature,  $\sim 298$  K) [11,23] and the substrate was established through a Peltier device mounted under the substrate as a heater. Single-molecule junctions were created following the same electrical conductance measurement. Once the conductance plateau was determined, the tip would be hovered with the tip/substrate distance maintained. Then we cut off the bias voltage and the current amplifier and switched the thermovoltage monitoring circuit by a voltage amplifier to directly record for a period of 100 ms. The thermopower of the molecular junction is given by Eq. 1 [24]:

$$S = S_{\text{cu}} - \Delta V_{\text{th}} / \Delta T \quad (1)$$

To obtain a statistical distribution of  $\Delta V_{\text{th}}$  of an Au-Molecule-Au junction, four temperature differences ( $\Delta T = 0, 5, 10$  and  $15$  K)

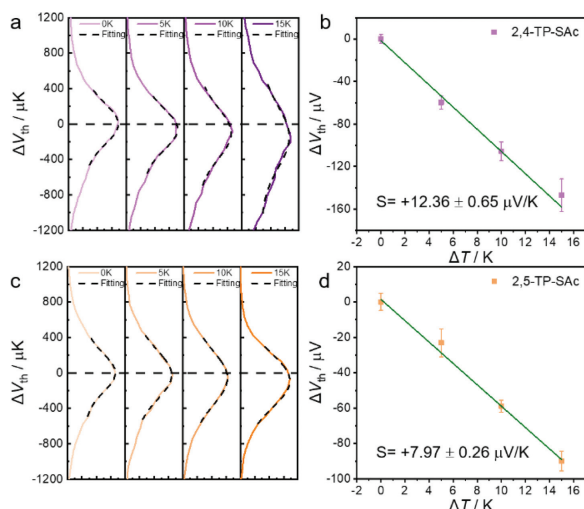


**Fig. 3.** (a, c) Histograms of 2,4-TP-SAC and 2,5-TP-SAC thermoelectric voltage measurements. Gaussian fits plotted in black short dash line. The black dash line indicates the baseline of thermoelectric voltage at  $\Delta V_{th} = 0$ . (b, d) The Seebeck coefficients were obtained from the thermovoltage as a function of  $\Delta T$ . Solid lines are linear fitting.

were given to perform thermopower measurements. Because the fluctuation of the molecular junction configurations inevitably occurs during the measurement process, the thermoelectric voltage from different molecular junctions formed during each tip hovering process might exhibit different distributions [20]. Thus, more than 1000 junctions' thermoelectric voltage values were recorded and summarized into histograms to obtain the most probable thermoelectric voltage during thermovoltage measurements. Typical histograms of the thermoelectric voltage for 2,4-TP-SAC and 2,5-TP-SAC are shown in Figs. 3a and c. The histogram peaks, which were based on the Gaussian fitting, representing the most probable measured  $V_{peak}$ , were chosen and plotted as a function of  $\Delta T$ , and the Seebeck coefficient was obtained from the thermoelectric slope in Figs. 3b and d. It can be seen that the Seebeck coefficients for 2,4-TP-SAC, 2,5-TP-SAC, 2,5-TP-Py and *para*-OPE3 are  $+12.36 \pm 0.65 \mu\text{V/K}$ ,  $+7.97 \pm 0.26 \mu\text{V/K}$ ,  $-7.56 \pm 0.69 \mu\text{V/K}$  and  $+7.78 \pm 0.34 \mu\text{V/K}$  in Table 1, respectively. The positive Seebeck coefficients for all three SAC-terminated molecules suggest that the dominated charge transport channel of them is the HOMO level [25]. However, the negative Seebeck coefficient of pyridine-terminated 2,5-TP-Py indicates that its dominated charge transport channel is the LUMO level, which has been verified in the previous work [12]. The results show that the thermopower of 2,4-TP-SAC with DQI is nearly twice of that of 2,5-TP-SAC without DQI. Moreover, we found the value of thermopower is almost the same for 2,5-TP-Py and *para*-OPE3 in the control experiment (Fig. S2 in Supporting information), suggesting that altering the anchor group and central thiophene core has little effect on the thermopower in this system. The QI effect is responsible for the increase of thermopower in single-molecule junctions.

To understand the influence of the DQI on the thermopower and charge transport on single-molecule junctions, we optimized structures for 2,4-TP-SAC and 2,5-TP-SAC (Fig. 4a) and investigated the transmission coefficient of electrons transferring between electrodes based on DFT calculations combined with non-equilibrium Green function (NEGF) to evaluate the changes originated from the DQI effect within the junctions (see Supporting information for more computational details) [26,27].

As the results (Fig. 4b), a distinct anti-resonance peak is observed within the HOMO-LUMO gap of the 2,4-TP-SAC junction, indicating the presence of DQI. While for 2,5-TP-SAC junction, the

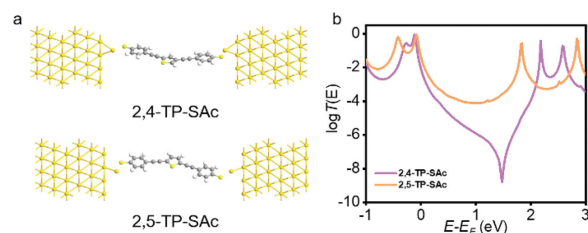


**Fig. 4.** (a) Optimized structures for 2,4-TP-SAC and 2,5-TP-SAC. (b) Theoretical transmission curves for Au-2,4-TP-SAC-Au junction (purple) and Au-2,5-TP-SAC-Au junction (orange).

transmission function exhibits a typical CQI feature, leading to higher conductance compared with the 2,4-TP-SAC junction. Within the range of the energy level gap, the 2,5-TP-SAC junction exhibits a higher transmission coefficient than the 2,4-TP-SAC junction, which is consistent with the experimental results. Besides, the steeper slope of the 2,4-TP-SAC junction is expected to higher Seebeck coefficient, while the 2,5-TP-SAC junction corresponds to a lower Seebeck coefficient, which agrees with experimental results. To further illustrate the DQI enhanced thermopower, we compare two types of molecules without DQI, which share a similar magnitude of Seebeck coefficient (Fig. S3 in Supporting information). Since the Fermi level is closer to the HOMO level for SAC-terminated molecular junctions, indicating that the electron transport through junctions is dominated by the HOMO level, thus further verify the positive Seebeck coefficient measured in the experiment. While for pyridine-terminated molecules 2,5-TP-Py, the negative Seebeck coefficient is originated from the LUMO-dominated transmission, which is consistent with the molecular energy spectrums (Figs. S3-S5 in Supporting information).

In conclusion, we have investigated thermopower and charge transport properties through single-molecule thiophene junctions using a modified STM-BJ technique. Two orders of magnitude lower conductance were observed between the 2,4-TP-SAC with DQI and 2,5-TP-SAC without DQI. The thermopower results provide experimental evidence of thermoelectric performance arising from DQI, which is also supported by the control experiment and DFT calculations. Our results reveal that QI effects are a promising strategy for the design of thermoelectric devices and materials with high thermopower.

#### Declaration of competing interest

The authors declare that they have no known competing financial interests or personal relationships that could have appeared to influence the work reported in this paper.

#### Acknowledgments

This work was supported by the National Natural Science Foundation of China (Nos. 21722305, 21933012, 31871877), the National Key R&D Program of China (No. 2017YFA0204902), the Fundamental Research Funds for the Central Universities (Nos. 20720200068, 20720190002), the National Science Foundation of Shanghai (No. 20ZR1471600), the Science and Technology Commission of Shanghai Municipality (No. 19DZ2271100), Natural Science Foundation of Fujian Province (No. 2018J06004), and the Beijing National Laboratory for Molecular Sciences (No. BNLM202005).

#### Supplementary materials

Supplementary material associated with this article can be found, in the online version, at doi:10.1016/j.ccl.2021.06.052.

**References**

- [1] B. Russ, A. Glauddell, J.J. Urban, et al., *Nat. Rev. Mater.* 1 (2016) 16050.
- [2] J. Liu, X. Huang, F. Wang, W. Hong, *Acc. Chem. Res.* 52 (2019) 151–160.
- [3] D. Xiang, X. Wang, C. Jia, et al., *Chem. Rev.* 116 (2016) 4318–4440.
- [4] C.J. Lambert, H. Sadeghi, Q.H. Al-Galiby, *C. R. Phys.* 17 (2016) 1084–1095.
- [5] C.M. Guédon, H. Valkenier, T. Markussen, et al., *Nat. Nanotechnol.* 7 (2012) 305–309.
- [6] J. Bai, A. Daaoub, S. Sangtarash, et al., *Nat. Mater.* 18 (2019) 364–369.
- [7] M.H. Garner, H. Li, Y. Chen, et al., *Nature* 558 (2018) 415–419.
- [8] X. Liu, S. Sangtarash, D. Reber, et al., *Angew. Chem. Int. Ed.* 56 (2017) 173–176.
- [9] K.G.L. Pedersen, A. Borges, P. Hedegård, et al., *J. Phys. Chem. C* 119 (2015) 26919–26924.
- [10] M. Paulsson, S. Datta, *Phys. Rev. B* 67 (2003) 241403.
- [11] P. Reddy, S.Y. Jang, R.A. Segalman, A. Majumdar, *Science* 315 (2007) 1568–1571.
- [12] J.R. Widawsky, P. Darancet, J.B. Neaton, L. Venkataraman, *Nano Lett.* 12 (2012) 354–358.
- [13] M. Buttiker, Y. Imry, R. Landauer, S. Pinhas, *Phys. Rev. B* 31 (1985) 6207–6215.
- [14] P.N. Butcher, *J. Phys. Chem.* 2 (1990) 4869–4878.
- [15] R. Miao, H. Xu, M. Skripnik, et al., *Nano Lett.* 18 (2018) 5666–5672.
- [16] A. Borges, G.C. Solomon, *J. Phys. Chem. C* 121 (2017) 8272–8279.
- [17] Y. Yang, M. Gantenbein, A. Alqorashi, et al., *J. Phys. Chem. C* 122 (2018) 14965–14970.
- [18] M.E. Cinar, T. Ozturk, *Chem. Rev.* 115 (2015) 3036–3140.
- [19] X. Li, Q. Wu, J. Bai, et al., *Angew. Chem. Int. Ed.* 59 (2020) 3280–3286.
- [20] H. Chen, S. Sangtarash, G. Li, et al., *Nanoscale* 12 (2020) 15150–15156.
- [21] B. Xu, N.J. Tao, *Science* 301 (2003) 1221–1223.
- [22] W. Haiss, H. van Zalinge, S.J. Higgins, et al., *J. Am. Chem. Soc.* 125 (2003) 15294–15295.
- [23] L. Shi, A. Majumdar, *J. Heat Transfer.* 124 (2002) 329–337.
- [24] G. Yzambart, L. Rincón-García, A.A. Al-Jobory, et al., *J. Phys. Chem. C* 122 (2018) 27198–27204.
- [25] K. Baheti, J.A. Malen, P. Doak, et al., *Nano Lett.* 8 (2008) 715–719.
- [26] C. Tang, L. Chen, L. Zhang, et al., *Angew. Chem. Int. Ed.* 58 (2019) 10601–10605.
- [27] Z.Q. Fan, K.Q. Chen, *Appl. Phys. Lett.* 96 (2010) 053509.